Advances in Science and Technology Research Journal

Advances in Science and Technology Research Journal 2024, 18(3), 188–199
https://doi.org/10.12913/22998624/186473
ISSN 2299-8624, License CC-BY 4.0

Received: 2024.03.07
Accepted: 2024.03.25
Published: 2024.04.20

Stability of Thin-Walled Composite Structures with Closed Sections Under Compression

Kuba Rosłaniec[1], Patryk Różyło[1*]

[1] Department of Machine Design and Mechatronics, Faculty of Mechanical Engineering, Lublin University of Technology, Nadbystrzycka 36, 20-618 Lublin, Poland

* Corresponding author's e-mail: p.rozylo@pollub.pl

ABSTRACT

The purpose of the research was to analyze the experimental-numerical influence of the type of cross-section on the stability of thin-walled composite columns with closed (rectangular) cross-sections. The subject of the investigation was thin-walled composite structures made of CFRP composite (carbon fiber reinforced polymer), characterized by a closed rectangular cross-section shape of the profile and a identical ply configuration. In this study, experimental and numerical investigations of axially compressed columns were performed to determine the values of buckling loads and buckling forms. Experimental investigations were performed using a universal testing machine with an optical deformation measurement system. In parallel with the experimental tests, numerical simulations were made using the Finite Element Method (FEM). The numerical studies conducted using dedicated numerical models and the experimental studies made it possible to carry out a thorough analysis of the impact of the cross-sectional shape on the buckling phenomenon of the structure. The novelty of the present paper is the use of interdisciplinary testing methods to compare the effect of cross-sectional geometry on the stability of thin-walled composite columns.

Keywords: buckling; closed composite profiles; experimental studies; numerical simulations; axial compression.

INTRODUCTION

Thin-walled columns, belong to the group of load-bearing elements, characterized by high stiffness as well as strength, while maintaining low self-weight [1, 2, 3]. Typically, these types of structures are made of GFRP (Glass Fiber Reinforced Polymer) – type composite material [4, 2] or CFRP (Carbon Fiber Reinforced Polymer) [5] [6]. There are two main types: with closed [7, 8] [9] and opens sections [10, 11, 12]. These structures, specifically with closed sections, are designed to carry loads, mainly compressive. They are commonly used in the aerospace, automotive and construction industries. They are subject to loss of stability – so called buckling. The above phenomenon results from the axial compression of the structure, consisting of deformation under the influence of a buckling load (the force necessary for the formation of the buckling mode), resulting in a rapid redistribution of internal stresses, which can result in the failure of the material [13, 14]. In most cases, thin-walled composite columns are capable of carrying compressive load after losing stability. Some structures are characterized by a load carrying capacity several times higher than the value of the buckling load (causing the buckling effect). As the compressive force increases, post-buckling incidences such as damage initiation, damage propagation and delamination – up to the failure – are observed once the buckling load is exceeded [15, 16, 17]. However, this paper will consider only the buckling state of composite structures.

The configuration of fiber orientation, the number of layers and the geometry of the composite profile directly influence the stiffness and strength characteristics of the structure and its response during loading [18, 19, 20]. In addition, the paper [21] presented the properties of

FML-type composite material in the context of material behavior depending on the layup of the composite material. An analysis of the buckling is carried out to determine the buckling form and buckling load. The value of buckling load is determined in experimental studies using approximation methods, which allow to estimate the buckling load from the equilibrium path which allows to estimate the forces at which the stability of the structure is lost [22, 23, 24]. In addition, the paper [25] presents the buckling problem in depth in terms of both experimental studies and numerical simulations, while the paper [26] presents the buckling problem in terms of analytical solutions. Methods for determining buckling loads for experimental studies have been presented in many papers, e.g. [18, 25, 27]**.** In numerical analyses based on the FEM, the buckling load and the nature of buckling state are determined from a linear analysis of the eigenproblem, using the criterion of minimum potential energy [18, 23]**.**

This article focuses on the comparison analysis of buckling forms and buckling loads of three different types of composite columns with identical ply configurations, different cross-sectional geometries, made of CFRP composite. Evaluation of the behavior of axially compressed composite profiles requires the use of some testing methods. Experimental tests were performed using a universal testing machine (UTM) as well as an optical deformation measurement system ARAMIS 2D [10, 28, 29]. Numerical simulations were conducted using the FEM in the software Abaqus®. The material properties of the analyzed structures were determined experimentally in the following works [30, 31].

Within the framework of commonly published results from the literature, the issue of stability and load carrying capacity primarily concerns composite structures with open sections. In this paper, the main focus is on composite profiles with closed sections – which demonstrate distinct behavior in both buckling and post-buckling states, which is the subject of current research. The novelty of this study is the comparison of the values of forces causing loss of stability and the character of buckling for three types of composite columns with closed sections using multiple independent test methods (use as follows: UTM, optical strain measurement system, numerical FEM simulations) and comparison of the results from experimental methods with numerical models dedicated to the profiles. The main objective of the research was to compare the values of loads and the character of buckling of three types of sections.

RESEARCH OBJECT

The objects of the research were thin-walled composite columns consisting of 8 layers, made of carbon epoxy composite CFRP [32, 33]. This article compares buckling forms and buckling load for 3 different types of profiles with a wall thickness equal 1.24 mm, a height of 200 mm and the following cross-sectional dimensions: A 40×40 mm, B 50×30 mm, C 60×20 mm. The following symmetrical stacking sequence was used in the tests $[0°/45°/-45°/90°]_s$. Both the material from which the composite profiles were made, as well as the number of layers and the selected layup of the laminate, were dictated by the preliminary assumptions of a research project from the National Science Centre – No. 2021/41/B/ST8/00148. Preliminary numerical simulations made it possible to select an appropriate arrangement of layers to obtain the full number of half-waves in the analysis of the structural stability issue. For each type of section, were made three real specimens and subjected to axial compression, a total of nine composite columns (A1_1, A1_2, A1_3, B1_1, B1_2, B1_3, C1_1, C1_2, C1_3) were used in the experimental study, which were made by autoclave technique using tape prepreg CYCOM 985-42%-HS-135-305. The 305 mm wide tape was characterized by a 42% by volume resin content of type 985 and a reinforcement made of carbon fiber of density 135 g/m^2. The composite columns were made by winding the prepreg around the inner core at an angle corresponding to the ply configuration. The autoclave curing parameters were: temperature 177 °C and pressure 0.6 MPa

Experimental studies made it possible to collect the equilibrium paths of the loaded structures, which allows for determine the buckling load values. During these tests, the buckling forms of the structures were registered using an ARAMIS 2D system. Numerical simulations, carried out with the commercial Abaqus® software using the FEM, made it possible to determine the force and buckling form by solving a linear eigenproblem. The material parameters used in the numerical studies were determined using the procedure outlined in the publication) [30]. The properties of the test material are shown in Table 1.

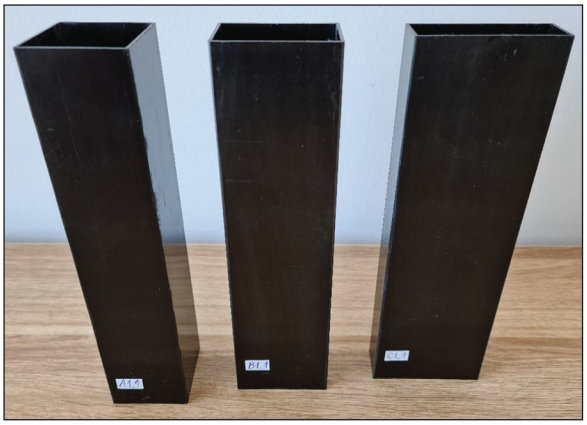

Figure 1. Example test samples

EXPERIMENTAL STUDIES

Experimental tests were performed using a UTM Zwick Z100 [18] [33]. Studies of the buckling of an axially compressed thin-walled composite structure were conducted at a constant feed rate of the testing machine head of 1 mm/min at a constant room temperature. In order to determine the value of the buckling force, the approximation method known as intersection of straight lines based on experimentally determined curves of the load-displacement relationship (shortening) was used [27] [34]. This method is based on the approximation of two characteristic, appropriately selected, sections (segments) of the experimental characteristics (curves) by means of a linear function. One of the selected curves must be before the change in the „stiffness" of the structure, and the other after the change in the „stiffness" of the structure, the selected curves must be approximated using a straight line. The point of crossing of straight lines, approximated sections of the experimental curve, corresponds to the approximate value of the buckling load and displacement at which the buckling effect occurred [27].

In order to verify the findings obtained through the method of straight lines, it is necessary to determine the value of the correlation coefficient known as R^2, which determines the correctness of the approximation of the selected sections from experimental studies. This coefficient is a trend line formula, which takes values that are closest to the experimentally obtained data (within the selected approximation ranges). The obtained approximation of the buckling load is acceptable when the value of the R^2 coefficient reaches a minimum of ≥ 0.95 agreement with the selected curve course. A higher value of the R^2 (the maximum value of approximation is 1) indicates greater accuracy of the obtained result [25] [27]. The „matrix method" was used to determine the buckling value [27], reduced to the formulation of the following system of equations 1:

$$\begin{cases} A_1 x + B_1 y + C_1 = 0 \\ A_2 x + B_2 y + C_2 = 0 \end{cases} \quad (1)$$

where: A_1 i A_2 – values of directional coordinates of the line x; B_1 i B_2 – values of directional coordinates of the line y; C_1 i C_2 – numerical values specifying free expression of the function.

In order to determine the intersection point (buckling value), equation 1 must be transformed into the form 2:

$$\begin{cases} A_1 x + B_1 y = -C_1 \\ A_2 x + B_2 y = -C_2 \end{cases} \quad (2)$$

The above system of first-degree equations (with two unknowns) can be solved by applying the matrix (determinant) method as follows:

$$W = \begin{vmatrix} A_1 & B_1 \\ A_2 & B_2 \end{vmatrix} = A_1 \times B_2 - A_2 \times B_1 \quad (3)$$

$$W_X = \begin{vmatrix} -C_1 & B_1 \\ -C_2 & B_2 \end{vmatrix} (-C_1) \times B_2 - (-C_2) \times B_1 \quad (4)$$

$$W_Y = \begin{vmatrix} A_1 & -C_1 \\ A_2 & -C_2 \end{vmatrix} (-C_2) \times A_1 - A_2 \times (-C_1) \quad (5)$$

When the above equations are nonparallel ($W \neq 0$), the equation system takes the following solution (6):

Table 1. Material properties of the CFRP – average values (standard deviation) [30]

Mechanical properties			Strength parameters		
Young's modulus E_1	MPa	103014.11 (2145.73)	Tensile strength F_{tu} (0°)	MPa	1277.41 (56.23)
Young's modulus E_2		7361.45 (307.97)	Compressive strength F_{cu} (0°)		572.44 (46.20)
Poisson's ratio v_{12}	-	0.37 (0.17)	Tensile strength F_{tu} (90°)		31.46 (9.64)
Kirchhoff modulus G_{12}	MPa	4040.53 (167.35)	Compressive strength F_{cu} (90°)		104.04 (7.34)
-		-	Shear strength F_{su} (45°)		134.48 (2.71)

$$\begin{cases} x = \dfrac{W_x}{W} \\ y = \dfrac{W_y}{W} \end{cases} \tag{6}$$

where: x and y denote the coordinates of the intersection point of two straight lines, that is the coordinates of the buckling point.

Experimental studies also used the ARAMIS 2D optical deformation measurement system, using the digital image correlation (DIC) method [35] [36] [37] [38]. This system makes it possible to observe and measure the deformations that happen when a thin-walled composite structure loses stability. The test stand is presented at Figure 2. W An LED lamp was used to correctly register the deformation, in order to correctly illuminate the sample and eliminate uneven illumination of the structure, which adversely affects the quality of deformation registration. The brightness of the lamp was selected to avoid unwanted overexposure of the recorded image. The unwanted effects of overexposure were eliminated by using a dedicated background to absorb the overexposure. The experimental specimens were placed in the center of the flat surfaces of the testing machine heads parallel to each other. The loading and shortening of the specimen realized by the traverse displacement was recorded in real time, making it possible to determine the buckling load value.

NUMERICAL SIMULATIONS

Numerical studies were carried out using the FEM with the commercial software Abaqus®. Dedicated numerical models were developed, taking into consideration the orthotropic Lamin-type material model (the model used the material parameters shown in Table 1), used for composite materials. The prepared models enabled a detailed analysis of the buckling of the structure based on the criterion of minimum potential energy, which allows for determine the force and buckling mode of the structure. The equation enabling the determination of the buckling load is presented below, in te resarch [8, 39] presents a detailed description of the solution:

$$(K_0^{NM} + \lambda_i K_\Delta^{NM}) v_i^M = 0 \tag{7}$$

where: K_0^{NM} – structural stiffnes matrix relating to the baseline (equivalent to the baseline condition, which includes the effects of preloads P^N), K_Δ^{NM} – the differential matrix of initial stress as well as load stiffness resulting from the incremental loading pattern (Q^N), λ_i – present the eigenvalues: v_i^M – the buckling (form) mode, known as the eigenvectors Normalized vectors, where the maximum displacement component is 1.0, ^{M} and ^{N} – the degrees of freedom of the entire model, i – buckling form (mode). The buckling load is represented by the following equation: $P^N + \lambda_i Q^N$.

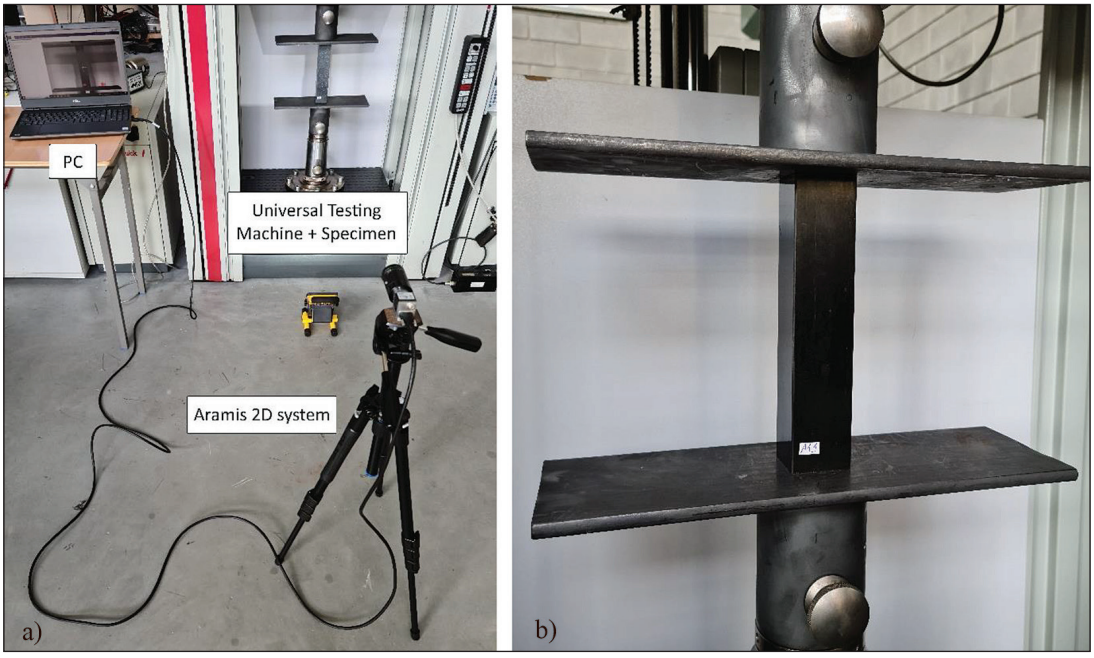

Figure 2. Experimental stand: a) general view of test stand, b) heads with composite column

The analyzed composite structures are made up of 8 layers of CFRP composite with the following layer arrangement $[0°/45°/-45°/90°]_s$. Discrete models were modeled using the Continuum Shell technique as SC8R-type finite elements, that is eight-node elements, having three degrees of freedom (translations) at each node. The machine's traverses were modeled as non-deformable planes (plates) using R3D4 four-node three-dimensional shell elements having four nodes and six degrees of freedom (three translational and three rotational). The discrete model of the composite columns consisted of 9200 finite elements, assuming a global mesh density of 2 mm. In contrast, the discrete model of non-deformable plates consisted of 1120 finite elements, with a global mesh density of 2.5 mm. The contact relations [40, 41] between the column and the plates were modeled with contact interactions in the tangential direction and in the normal direction with frictional force (friction coefficient = 0.2). Boundary conditions were modeled using reference points coupled to non-deformable plates. In order to represent the operation of the universal testing machine, all degrees of freedom of the bottom plate (translational and rotational) were fixed (blocked), while the top plate, realizing compression of the structure, was left free in the translational direction on the Z-axis, making it possible to apply the load to the reference point of this plate, thus realizing compression of the structure with respect to the Z-axis. The above-described numerical model was used to identify the buckling load and buckling form values using the finite element method of three types of 8-layer composite columns made of CFRP with identical composite layer configurations $[0°/45°/-45°/90°]_s$, with different in cross-sectional profile: A 40×40 mm, B 50×30 mm, C 60×20 mm. An example of a discrete model is shown in the figure below.

More details on numerical simulations are presented in the paper [33]. All analysis was carried out in Abaqus due to the fact that this was one of the objectives of the project from the National Science Centre (2021/41/B/ST8/00148) under which this publication was developed.

RESEARCH RESULTS

Experimental tests conducted made it possible to define the buckling phase of the loaded columns. The value of buckling forces was determined using the straight line method on the basis of the results recorded using a UTM. Figures 4, 5, and 6 graphically show the method of determining the buckling load for nine samples. The lines shown in the following figures indicate: black solid line – experimental curve, black dashed line – buckling load, red solid line – effective approximation range, and red dashed line – approximation function.

The determined values of buckling loads made it possible to compare the impact of the type of cross-section on the buckling of the structure made of fiber composite. In order to better show

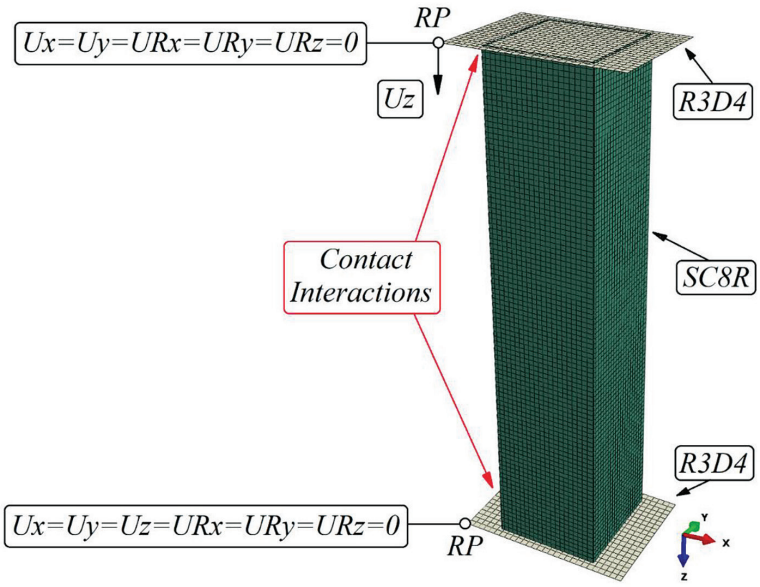

Figure 3. Discrete model with defined boundary conditions

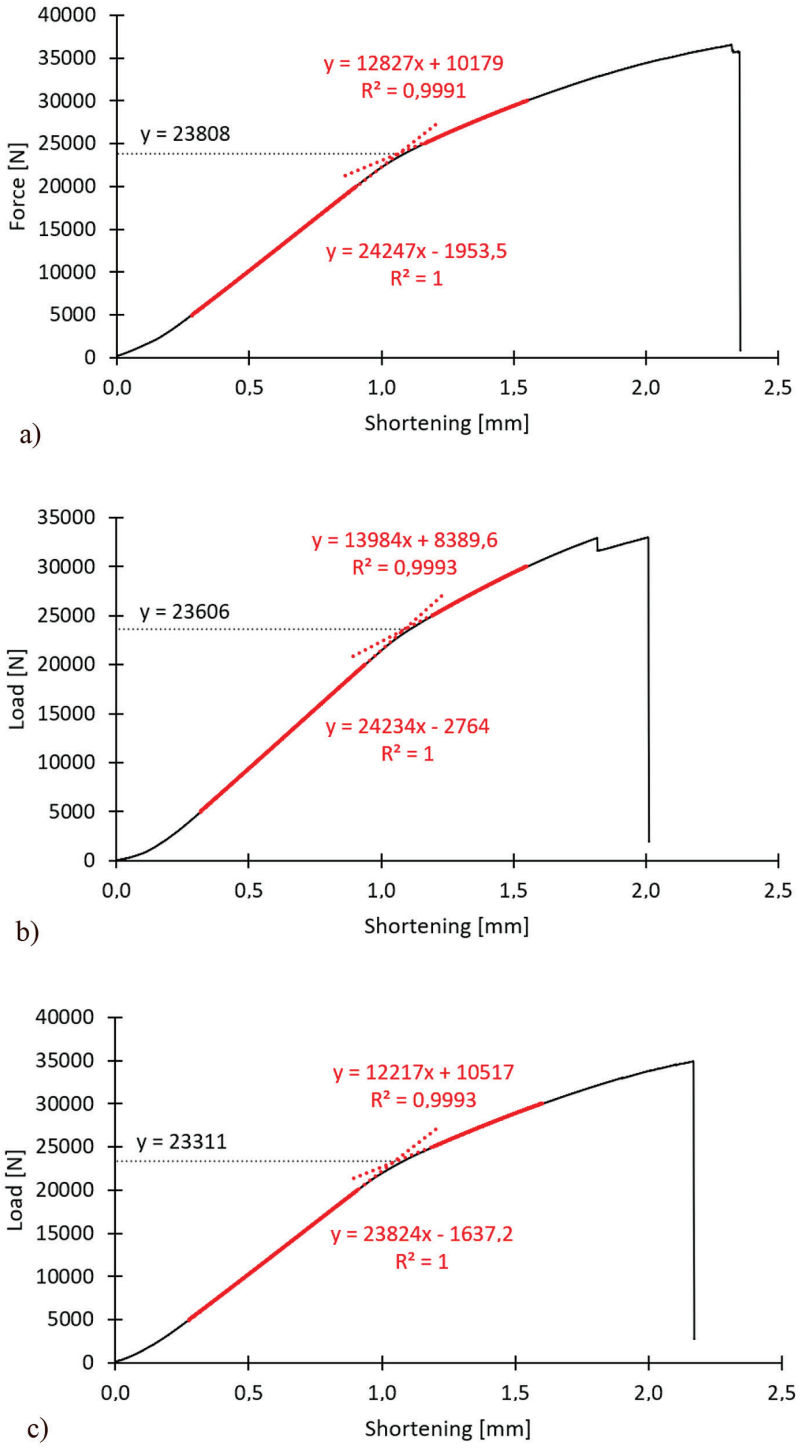

Figure 4. Experimentally determined buckling force: (a) specimen A1_1, (b) specimen A1_2, (c) specimen A1_3

and compare the results, the results for 3 types of cross-section were collected and are presented in the Table 2. It was shown that the A1 profile had the highest load value at which the buckling (buckling state) of the structure occurs. The average value of the buckling force for the profiles was: A1 – 23575 N, B2 – 19828 N and C1 – 14779 N. Comparing the average results, it was found that the average buckling load, for the A1 type profile, is nearly 1.60 times higher than the average buckling force of the C1 profile. It was also observed that buckling of the column occurs at different values of shortening. The average value of shortening of the column was for each type of profile: A – 1.06 mm, B – 0.91 mm, C – 0.72 mm. The largest difference in shortening was between

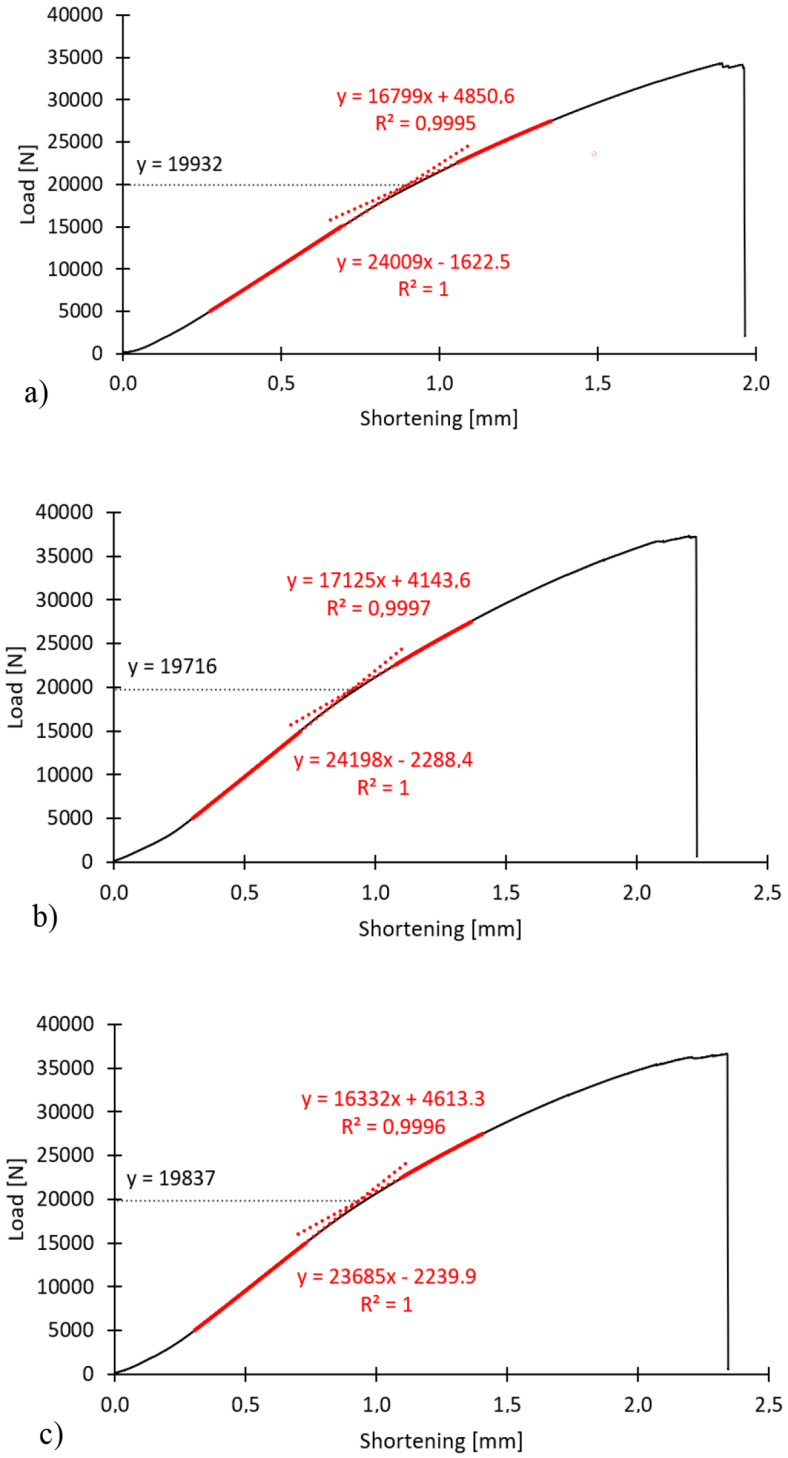

Figure 5. Experimentally determined buckling force: (a) specimen B1_1, (b) specimen B1_2, (c) specimen B1_3

the type A and C profiles, it was 0.34 mm about 47%. It has been found that the geometry of the cross-section of the column has a significant effect on the value of the buckling force and the shortening that occurs during buckling. The buckling forms were registered experimentally using the Aramis 2D DIC. The use of special filters (median filters) highlighting the deformations made it possible to capture the buckling form and graphically represent the buckling of the actual structure. The recorded buckling forms are shown in the Figure 7. Parallel numerical studies of the buckling of the structure made it possible to determine the strength and buckling form of the analyzed types of structures. The results obtained using the finite element method are presented in

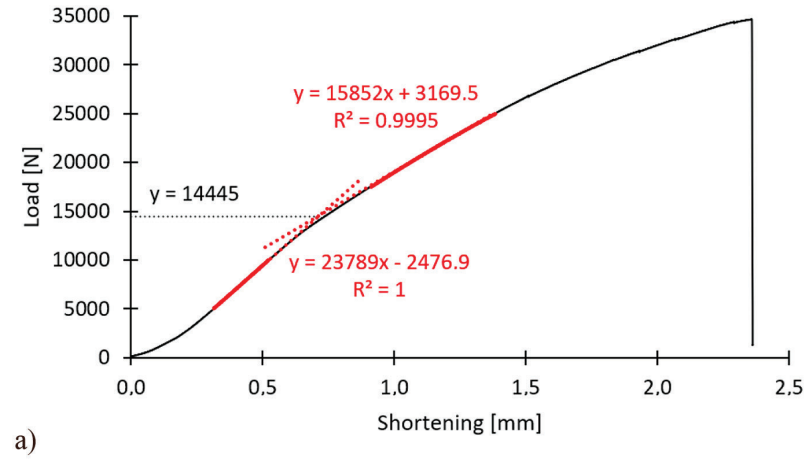

a)

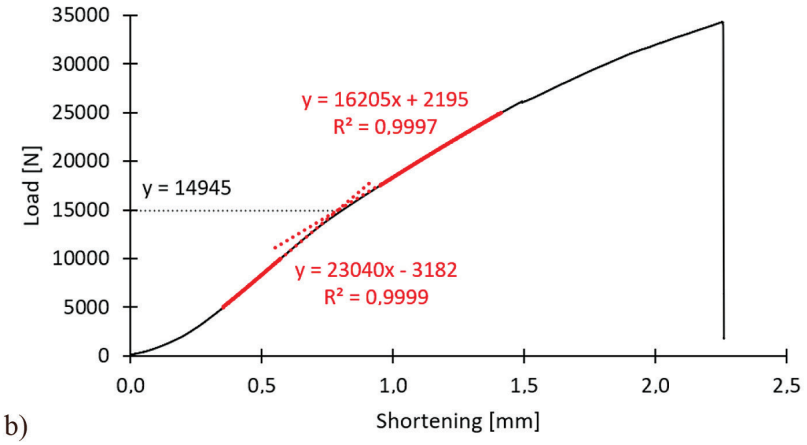

b)

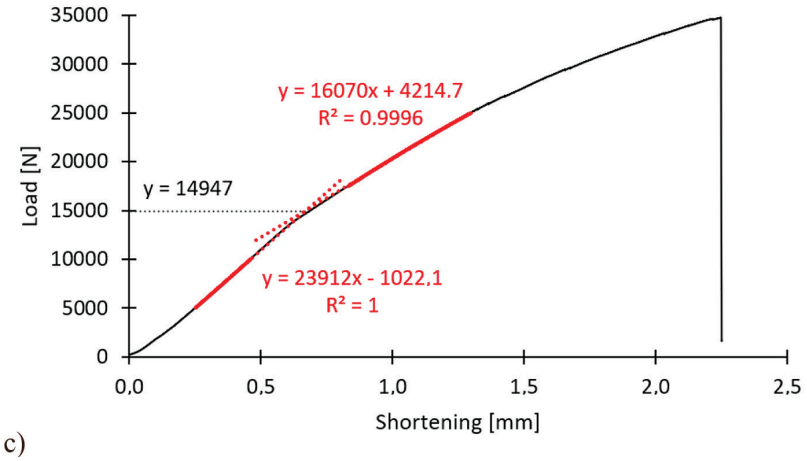

c)

Figure 6. Experimentally determined buckling force: (a) specimen C1_1, (b) specimen C1_2, (c) specimen C1_3

the Figure 8. The values of buckling forces obtained in numerical and experimental analyses have a high level of agreement both qualitatively and quantitatively. In the experimental tests, it was observed that for different types of composite column cross-sections there is a certain number of half-waves (in the longitudinal direction): A1 – four half-waves, B1 – three large half-waves, C1 – three large half-waves. The experimentally obtained buckling forms coincide with the results of the finite element method. The small differences in the obtained results between the experimental and simulation methods testify to the correct execution of the research. The results obtained by numerical simulations show an unknown higher value compared to the experimental results, the

Table 2. Comparison of buckling force values obtained by experimental method

Specimen type	Specimen No.			Averange value
	1	2	3	
A1	23808 N	23606 N	23311 N	23575 N
B1	19932 N	19716 N	19837N	19828 N
C1	14445 N	14945 N	14947 N	14779 N

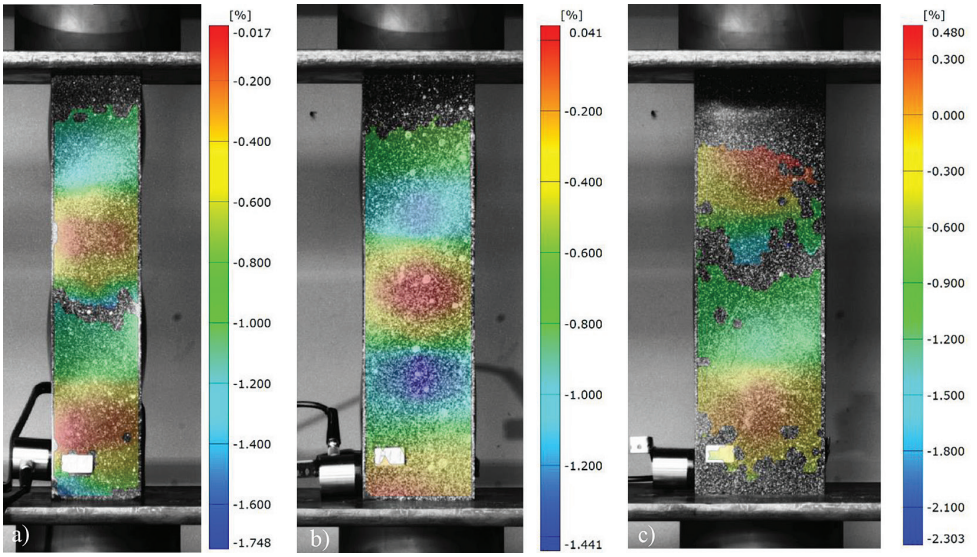

Figure 7. Loss of stability (buckling) - experimental tests: (a) specimen A1_1, (b) specimen B1_1 (c) specimen C1_1

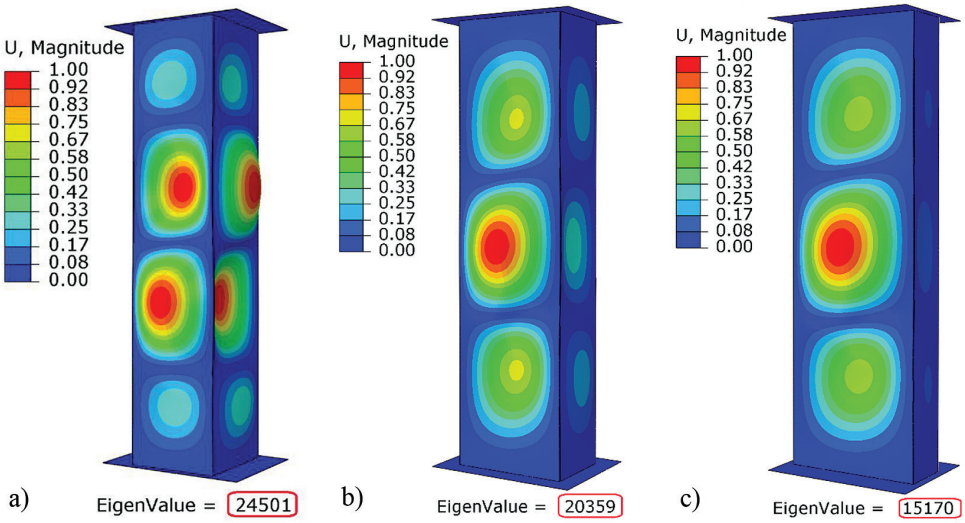

Figure 8. Loss of stability (buckling) - numerical simulations: (a) specimen A1, (b) specimen B1, (c) specimen C1

maximum difference was 3.92%. This is due to the fact that the physical models analyzed in the numerical simulations were idealized, devoid of geometric imperfections resulting from the process and technology of manufacturing composite columns. A comparison of the obtained results is presented in Table 3. Regarding the results obtained, it was observed that the use of the approximation method of intersection of straight lines, makes it possible to determine the values of buckling loads based on the experimental load-shortening (displacement) curve. Correct selection of

Table 3. Buckling results—comparison of experimental and numerical investigations

Specimen type	EXP experimental average value	FEM value	FEM/EXP
A1	23575 N	24501 N	1.04
B1	19828 N	20359 N	1.03
C1	14779 N	15170 N	1.03

the approximation range (both the part before and after the change in the „stiffness" of the experimental curve allows to determine the values of buckling loads with very high accuracy. When determining buckling loads regardless of the approximation method [24], it is necessary, first of all, to ensure that the approximated sections of the experimental curve show a correlation coefficient of at least 0.95 – as described in the paper [25]. On the basis of the study, it was observed that the results of buckling loads obtained by experimental testing, are slightly lower in value than those obtained by numerical simulations. The above, is due to the fact that actual specimens are, among other things, subject to geometric imperfections, while numerical models represent an ideal design.

CONCLUSIONS

This article presents a buckling state analysis of thin-walled composite profiles with closed cross sections made of CFRP. The study compares the effect of cross-sectional geometry of structures: A1 40×40 mm, B1 50×30 mm, C1 60x×20 mm characterized by equal height, summary of cross-sectional edge lengths and configuration of laminate layers $[0°/45°/-45°/90°]_s$. An interdisciplinary study using a universal testing machine (UTM), an optical deformation measurement system (ARAMIS 2D DIC) and numerical analyses made it possible to determine both the values of buckling loads and buckling forms for each analyzed structure. The study showed that the geometry of the cross-section, while maintaining a uniform arrangement of laminate plies, has a significant effect on the force and buckling form. It was observed that thin-walled structures characterized by a square cross-section are characterized by higher stability, compared to rectangular structures. The greater the disproportion between the lengths of the column sides, the structure is characterized by lower buckling strength. The value of the averaged buckling load, for the A1 type profile, is nearly 1.60 times higher than the average buckling force of the C1 profile and about 1.19 times higher than the average buckling load of the B1 profile. A high agreement is evident in both the qualitative and quantitative assessment of results, achieved through a combination of experimental and numerical methodologies. This indicates that it is possible to develop a discrete model that accurately represents the work of the real structure. The buckling load obtained by the computational method was higher by a maximum of 1.04 than the average value of the results obtained experimentally, the number of half-waves occurring in both methods was identical – the conclusion is for observations on the example of the A1 profile. The above studies do not exhaust the issue of buckling of thin-walled composite columns with closed sections. A further direction of research will be the post-buckling analysis of stressed structures up to complete failure, taking into account the damage criteria dedicated to composite materials [42, 43]. Future study will focus on comparing the behavior of structures in the post-buckling state, including damage initiation and propagation effects, up to the failure of structures.

Ackowledgments

The research was conducted under project No. 2021/41/B/ST8/00148, financed by the National Science Centre, Poland. This research was funded in whole or in part by National Science Centre, Poland [2021/41/B/ST8/00148]. For the purpose of Open Access, the author has applied a CC-BY public copyright license to any Author Accepted Manuscript (AAM) version arising from this submission.

REFERENCES

1. Swanson S.R. Introduction to Design and Analysis with Advanced Composite Materials, Englewood Cliffs: Prentice-Hall, 1997.
2. Fascetti A., Feo L., Nistic N. and Penna R. Web-flange behavior of pultruded GFRP I-beams: A lattice model for the interpretation of experimental results,

Composites Part B: Engineering 2016; 257–269, https://doi.org/10.1016/j.compositesb.2016.06.058

3. Różyło P., Falkowicz K., Wysmulski P., Dębski H., Paśnik J. and Kral J. Experimental-numerical faiure analysis of thin-walled composite columns using advanced damage models, Materials 2021; 14(6): 1506, https://doi.org/10.3390/ma14061506
4. Berardi V., Perrella M., Feo L. and Cricrì G. Creep behavior of GFRP laminates and their phases: Experimental investigation and analytical modeling, Composites Part B Engineering, pp. 136-144, 2017, 122. DOI: https://doi.org/10.1016/j.compositesb.2017.04.015
5. P. Rożyło and H. Dębski, Effect of eccentric loading on the stability and load-carrying capacity of thin-walled composite profiles with top-hat section, Composite Structures 2020; 245: 112388, https://doi.org/10.1016/j.compstruct.2020.112388
6. Różyło P., Rosłaniec K., and Kuciej M. Buckling of compressed thin-walled composite structures with closed sections, Advances in Science and Technology Research Journal 2023; 17(6): 63–72, https://doi.org/10.12913/22998624/174193
7. Kim N-I., Shin D.K. and Park Y.S. Coupled stability analysis of thin-walled composite beams with closed cross-section, Thin-Walled Structures 2010; 18(8): 581–596, https://doi.org/10.1016/j.tws.2010.03.006
8. Urbaniak M., Świniarski J., Czapski P. and Kubiak T. Experimental investigations of thin-walled GFRP beams subjected to pure bending, Thin-Walled Structures 2016, 107: 397–404, https://doi.org/10.1016/j.tws.2016.06.022
9. Droździel M., Podolak P., Czapski P., Zgorniak P. and Jakubczak P. Failure analysis of GFRP columns subjected to axial compression manufactured under various curing-process conditions, Composite Structures, 2011; 262: 113342, https://doi.org/10.1016/j.compstruct.2020.113342
10. Gliszczyński A. and Kubiak T. Progressive failure analysis of thin-walled composite columns subjected to uniaxial compression, Composite Structures 2017; 169: 52–61, https://doi.org/10.1016/j.compstruct.2016.10.029
11. Dębski H., Samborski S., Różyło P. and Wysmulski P. Stability and load-carrying capacity of thin-walled FRP composite Z-profiles under eccentric compression, Materials 2020; 13(13): 2956, https://doi.org/10.3390/ma13132956
12. Różyło P. Failure phenomenon of compressed thin-walled composite columns with top-hat cross-section for three laminate lay-ups, Composite Structures 2023; 304: 116381, https://doi.org/10.1016/j.compstruct.2022.116381
13. Baker A., Dutton S. and Donald K.D. Composite materials for aircraft structures, Reston: American Instituite of Aeronautics and Astronautics 2004.
14. Soutis C. Carbon fiber reinforced plastics in aircraft construction, Materials Science ang Engineering 2005, 412(1–2): 171–176, https://doi.org/10.1016/j.msea.2005.08.064
15. Zaczynska M. and Mania R.J. Investigation of dynamic buckling of fiber metal laminate thin-walled columns under axial compression, Composite Structure 2021; 17(4), https://doi.org/10.12913/22998624/169970
16. Li W., Cai H., Li C., Wang K. and Fang L. Progressive failure of laminated composites with a hole under compressive loading based on micromechanics, Advanced Composite Materials 2014; 23(5–6): 477–490, https://doi.org/10.1080/09243046.2014.915105
17. Banat D., Mania R.J. and Degenhardt R. Stress state failure analysis of thin-walled GLARE composite members subjected to axial loading in the post-buckling range, Composite Structure 2022; 289: 115468, https://doi.org/10.1016/j.compstruct.2022.115468
18. Różyło P. and Dębski H. Failure study of compressed thin-walled composite columns with top-hat cross-section, Thin-Walled Structures 2022; 180: 109869, https://doi.org/10.1016/j.tws.2022.109869
19. Zhang H., Yang D., Ding H., Wang H., Xu Q.Y. Ma and et al., Effect of Z-pin insertion angles on low-velocity impact mechanical response and damage mechanism of CFRP laminates with different layups, Composites Part A: Applied Science and Manufacturing 2022; 150: 106593, https://doi.org/10.1016/j.compositesa.2021.106593
20. Qiu C., Han Y., Shanmugam L., Zhao Y., Dong S., Du S. and et al. A deep learning-based composite design strategy for efficient selection of material and layup sequences from a given database, Composites Science and Technology 2022; 230: 109154, https://doi.org/10.1016/j.compscitech.2021.109154
21. Hu Y., Zhang Y., Fu X., Hao G. and Jiang W. Mechanical properties of Ti/CF/PMR polyimide fiber metal laminates with various layup configurations, Composite Structures 2019; 229: 111408, https://doi.org/10.1016/j.compstruct.2019.111408
22. Bin Kamarudin M.N., Mohamed Ali J.S., Aabid A. and Ibrahim Y.E., Buckling analysis of a thin-walled structure using finite element method and design of experiments, Aerospace 2022; 9(10): 541, https://doi.org/10.3390/aerospace9100541
23. Kubiak T. Static and dynamic buckling of thin-walled plate structures, Dordrecht, The Netherlands: Springer Science and Business Media LLC 2013; 112–121, http://dx.doi.org/10.1007/978-3-319-00654-3_3
24. Paszkiewicz M. and Kubiak T. Selected problems concerning determination of the buckling load of channel section beams and columns, Thin-Walled Structures 2015; 93: 112–121. https://doi.org/10.1016/j.tws.2015.03.009

25. Różyło P., Teter A., Dębski H., Wysmulski P. and Falkowicz K. Experimental and numerical study of the buckling of composite profiles with open cross section under axial compression, Applied Composite Materials 2017; 24(5): 125–11264, 10.1007/s10443-017-9583-y
26. Ragheb W.F.W.F. Local buckling analysis of pultruded FRP structural shapes subjected to eccentric compression, Thin-Walled Structures 2010; 48(9): 709–717, https://doi.org/10.1016/j.tws.2010.04.011
27. Kamarudin M.N.B., Ali J.S. Aabid M.A. and Ibrahim Y.E., Buckling analysis of a thin-walled structure using finite element method and design of experiments, Aerospace 2022; 9(10): 541, https://doi.org/10.3390/aerospace9100541
28. Rozylo P. and Falkowicz K., Stability and failure analysis of compressed thin-walled composite structures with central cut-out, using three advanced independent damage models, Composite Structures 2021; 273: 114298, https://doi.org/10.1016/j.compstruct.2021.114298
29. Kubiak T., Samborski S. and Teter A. Experimental investigation of failure process in compressed channel-section GFRP laminate columns assisted with the acoustic emission method, 2015; 133: 921–929, https://doi.org/10.1016/j.compstruct.2015.08.023
30. Różyło P., Smagowski W. and Paśnik J. Experimental research in the aspect of determining the mechanical and strength properties of the composite material made of carbon-epoxy composite, Advances in Science and Technology Research Journal 2023; 17(2): 232–246, https://doi.org/10.12913/22998624/161598
31. Różyło P., Determined material properties within the framework of the NCN project (OPUS) No. 2021/41/B/ST8/00148. Dataset.Source: Zenodo 2023; https://doi.org/10.5281/zenodo.7606941
32. Wysmulski P. Numerical and experimental study of crack propagation in the tensile composite plate with the open hole, Advances in Science and Technology Research Journal 2023; 17(4): 249–261, https://doi.org/10.12913/22998624/169970
33. Różyło P. and Dębski H. Stability and load carrying capacity of thin-walled composite columns with square cross-section under axial compression, Composite Structures 2024; 329: 117795, https://doi.org/10.1016/j.compstruct.2023.117795
34. Rozylo P., Rogala M. and Pasnik J. Buckling analysis of thin-walled composite structures with rectangular cross-sections under compressive load, Materials 2023; 16: 6835, https://doi.org/10.3390/ma16216835
35. Nowak M. and Maj M. Determination of coupled mechanical and thermal fields using 2D digital image correlation and infrared thermography: Numerical procedures and results, Archives of Civil and Mechanical Engineering 2018; 18(2): 630–644, https://doi.org/10.1016/j.acme.2017.10.005
36. Holmes J., Sommacal S., Das R., Stachurski Z. and Compston P. Digital image and volume correlation for deformation and damage characterisation of fibre-reinforced composites: A review, Composite Structures 2023; 315: 116994, https://doi.org/10.1016/j.compstruct.2023.116994
37. Reu P.L., Toussaint E., Jones E., Bruck H.A., Iadicola M., Balcaen R., Turner D.Z., Siebert T., Lava P. and Simonsen M. DIC challenge: developing images and guidelines for evaluating accuracy and resolution of 2D analyses, Experimental Mechanics 2018; 58: 1067–1099, http://dx.doi.org/10.1007/s11340-017-0349-0
38. Khoo S.-W., Karuppanan S. and Tan C.-S. A review of surface deformation and strain measurement using two-dimensional digital image correlation, Metrology and Measurment Systems 2016; 3: 461480, https://doi.org/10.1515/mms-2016-0028
39. Różyło P. Stability and failure of compressed thin-walled composite columns using experimental tests and advanced numerical damage models, International Journal for Numerical Methods in Engineering 2021; 122(18): 5076–5099.
40. Grzejda R. Fe-modelling of a contact layer between elements joined in preloaded bolted connections for the operational condition, Advances in Science and Technology Research Journal 2014; 8(24): 19–23, https://doi.org/10.12913/22998624/561
41. Grzejda R. Determination of bolt forces and normal contact pressure between elements in the system with many bolts for its assembly conditions, Advances in Science and Technology Research Journa 2019, 13(1): 116–121, https://doi.org/10.12913/22998624/104657
42. Różyło P., Dębski H. and Kral J. Buckling and limit states of composite profiles with top-hat channel section subjected to axial compression, AIP Conference Proceedings 2018; 122(1), https://doi.org/10.1063/1.5019072
43. Hu H., Niu F., Dou T. and Zhang H. Rehabilitation effect evaluation of CFRP-lined prestressed concrete cylinder pipe under combined loads using numerical simulation, Mathematical Problems in Engineering 2018; 3268962, https://doi.org/10.1155/2018/3268962